J Mater Sci: Mater Med (2008) 19:2809–2817
DOI 10.1007/s10856-008-3407-4

Evaluation of physical–chemical properties and biocompatibility of a microrough and smooth bioactive glass particles

Ariadne Cristiane Cabral da Cruz · Márcia Thaís Pochapski · Ricardo Tramonti · José Caetano Zurita da Silva · Augusto Celso Antunes · Gibson Luiz Pilatti · Fábio André Santos

Received: 15 July 2007 / Accepted: 7 February 2008 / Published online: 6 March 2008

Abstract The purpose of this study was to evaluate physical–chemical and biocompatibility characteristics of a simple synthesis and low cost experimental bioactive glass. Physical and chemical properties were analyzed using scanning electron microscopy (SEM), X-ray energy dispersive (EDX), X-ray fluorescence (XRF) and X-ray diffraction (XRD). The biomaterials were subcutaneously implanted into rats, according to the following groups: G1, PerioGlas™; G2, Biogran™, G3, Experimental Bioactive Glass U (BGU) and G4, Control (Sham). After 7, 15, 21, 45, and 60 days, 5 animals/group/period were sacrificed and the subcutaneous tissue was dissected for histological and histometric analysis, considering inflammatory reaction and granulation area, presence of polymorphonuclear (PMN), monuclear (MN) and fibroblast (F) cells. SEM analysis of biomaterials showed irregular particles with different surface characteristics. EDX showed calcium, oxygen, sodium, phosphorus and silicon; XRF revealed silica oxide (SiO_2), sodium oxide (Na_2O), calcium oxide (CaO) and phosphorus oxide (P_2O_5). XRD indicated non crystalline phase. Measurement of tissue reaction showed similar results among the experimental groups at 45 and 60 days. No difference was found for PMN, MN and F cell counts. All biomaterials exhibited partial resorption. In conclusion, the experimental bioactive glass analyzed showed physical and chemical characteristics similar to the commercially available biomaterials, and was considered biocompatible, being partially reabsorbed in the subcutaneous tissue.

A. C. C. da Cruz · M. T. Pochapski · G. L. Pilatti · F. A. Santos (✉)
Department of Dentistry, State University of Ponta Grossa, CEP-84030-900 Uvaranas, Ponta Grossa, PR, Brazil
e-mail: fasantos@uepg.br

R. Tramonti
Department of Histology, Federal University of Santa Catarina, Florianópolis, SC, Brazil

J. C. Z. da Silva · A. C. Antunes
Department of Chemistry, State University of Ponta Grossa, Ponta Grossa, PR, Brazil

1 Introduction

Several researchers have been trying to find an ideal biomaterial to be used as a bone substitute. Autogenous bone grafts (ABG) are most widely used by surgeons for ridge augmentation and the reconstruction of osseous defects [1–3]. The major disadvantages of ABG are donor site morbidity, limitations on the quantity of grafted materials and high costs [3–5]. Therefore, there was a critical need for the development of bone substitute materials that match the properties of bone without the drawbacks of autografts or allografts, being supplied at any time, in any amount and at lower costs [6, 7].

Considerable attention has been directed towards the use of synthetic grafts including hydroxyapatite (HA), tricalcium phosphate and bioactive glass [8–13]. Bioactive glasses (BG) are a class of biomaterials generally based on amorphous silicate compounds. These materials have been used alone or in combination with ABG as bone regenerative materials in dental and orthopedic applications [3, 14–16]. Bioactive glass granules implanted in bone tissue fully react to form internal silica gel cores (Si-rich) with calcium phosphate rich surface (Ca–P-rich). In this process, the internal silica gel core degrades, leaving an external calcium phosphate bulk. Inside the excavated granules, osteoprogenitor cells differentiate and form new

bone tissue which was not originated from the external surface of the granule or from pre-existing bone [17–19].

Physical–chemical characteristics are important aspects considering the biological properties of the bioactive glasses. The roughness of the biomaterial surface has been shown to exert a positive effect on the cellular response and new bone. A chemical etching method was developed to create a microrough surface on bioactive glass microspheres, which was shown to significantly enhance osteoblast attachment in vitro. The presence of crystalline phases, usually with high chemical stability, makes the formation of a silica gel layer in glass ceramics more difficult, with the glassy phase being solely responsible for bioactive behaviour [11, 18, 20, 21].

The purpose of this study was to investigate the physical–chemical properties and evaluate biocompatibility of a simple synthesis and low cost experimental bioactive glass with microrough and smooth particles and no chemical surface treatment.

2 Materials and methods

2.1 Porous glass synthesis and characterization:

The biomaterials tested were divided into three groups: Group 1 (G1) PerioGlas™ (US Biomaterials Corporation, Alachua, Florida, USA); Group 2 (G2) Biogran™ (Orthovita Palm Beach Gardens, Florida, USA). Group 3 (G3) Experimental bioactive glass—State University of Ponta Grossa (BGU). BGU was prepared from a glass powder mixture with a 45% SiO_2, 24.5% Na_2O, 24.5% CaO, 6% P_2O_5 nominal composition by weight. The glass components were premixed, melted in a platinum crucible for 24 h at 1350°C and poured into graphite moulds. The glass discs were cracked into pieces and mechanically reduced to small particles. Several size ranges of the particles were retained by sifting. No chemical surface treatment was made. These particles were cleaned ultrasonically in pure acetone, dried at room temperature and sterilized in steam autoclave (120°C/15 min/15 psi).

2.2 Particles characterization

2.2.1 Physical–chemical characterization

Physical–chemical characterization was done to evaluate the micro architecture, phase purity, crystallinity, composition and functional groups of bioactive glasses.

2.3 Scanning electron microscope (SEM)

The bioactive glass powders were gold coated in an ion sputter (Shimadzu C-50™) and the microstructure (shape and surface) was examined using SEM (JSM T330™ JEOL, Tokyo, Japan). Electron micrographs were obtained at ×100 and ×5000 magnification. The diameter of the granules (five samples for each group) was measured (Image Tool™ version 3.0 image analysis software, University of Texas Health Science Center, San Antonio, Texas, USA).

2.4 Energy-dispersive X-ray (EDX)

Qualitative information about the chemical elements in the samples was performed using EDX spectra set at 20 kV for 300 s (JEOL 8400™, Jeol, Tokyo, Japan).

2.5 X-ray fluorescence (XRF)

XRF spectrometry (XRF 700™ Shimadzu, Kyoto, Japan) was used to quantify the samples' chemical composition (Ca and P ratio). The data were acquired with an axial wavelength-dispersive XRF unit.

2.6 X-ray diffraction (XRD)

XRD (XRD-6000™, Shimadzu, Kyoto, Japan) spectra were measured by the powder diffraction method. The materials were scanned from 5° to 80° in 2 theta (θ) and then the diffraction peaks of G1 (PerioGlas™), G2 (Biogran™) and G3 (BGU) were used to determine the phase purity and crystallinity.

2.7 Biocompatibility analysis

A hundred male rats (*Rattus norvegicus*—Wistar), weighing approximately 300–400 g (3–4 months-old), were randomly divided into four groups (25 animals for each group): G1, PerioGlas™, G2, Biogran™, G3, BGU and G4, Sham. The study was carried out following the guidelines of the Ethics Committee for Teaching and Research in Animals (protocol n.1049/02).

The same surgical sequence was followed for all animals. The rats were anesthetized with an intraperitoneal injection (ketamine, 75 mg/kg and xylazine, 10 mg/kg). The dorsum of the animal, following the sagittal line, was submitted to trichotomy for exposure of the skin and a straight 18 mm-length incision was performed. The margins of the incisions were then retracted and the connective tissue was dissected for placement of 30 mg of biomaterial in each side (each animal received only one biomaterial). After material implantation, the margins of the wound were joined and closed with interrupted suture (3-0 silk sutures–Ethicon™, Johnson & Johnson S/A, São José dos Campos,

Brazil). All animals received normal diet and water ad libitum during the entire study period.

Animals were anesthetized and a specimen of reaction tissue containing the material was removed 7, 15, 21, 45 and 60 days after implantation. Thereafter, the animals were sacrificed by cervical displacement, according to the guidelines of the Brazilian College of Animal Experimentation (COBEA). The biopsies were fixed in 10% phosphate buffered formalin for 24 h, decalcified by Morse solution (1:1 of sodium citrate 20% and formic acid 50%) for 15 days, and embedded in paraffin. After histotechnical processing, 5 μm thick alternate sections were taken from each specimen and stained with hematoxylin-eosin stain.

Qualitative histological analysis was made at ×100 magnification (Leica™, Leica do Brasil, São Paulo, Brazil). The biological response was evaluated for inflammatory alterations (presence of edema, vascular alterations and inflammatory infiltrate), reparative process (degree of fibrosis, angioblastic and fibroblastic proliferation) of the tissues developed around the material and particles degradation. Tissue reaction (inflammatory infiltrate, reparative process and fibrous capsule) was also measured considering the first cell layer in contact with material until the first muscle cell layer. In the sham control group the tissue reaction was measured between the muscle tissue (×40 magnification). Particle area (reabsorbed) was measured in the same section (×100 magnification). Inflammatory cells (neutrophils, PMN and mononuclear cells, MN, including lymphocytes, plasma cells, monocytes, and macrophages) and fibroblasts (F) were counted. Inflammatory cells within the vessels were excluded. The cells were counted in five different areas of each histological sample (×400 magnification).

All the measurements were made by a single masked, previously calibrated operator using digital analysis software (Image Tool™ version 3.0 image analysis software, University of Texas Health Science Center, San Antonio, Texas, USA).

2.8 Statistical analysis

Intra-examiner reproducibility (particle area, tissue reaction, and cell counts) was tested with intraclass correlation coefficient (ICC). Comparisons among groups considering particle size (in vitro), inflammatory response, cell counts, and granule degradation after experimental periods were tested with ANOVA with Tukey post hoc test. The normality of distributions of data was confirmed by the Shapiro–Wilks test and the homogeneity of variances was evaluated using the Levene test. Prior to statistical analyses, logarithmic transformations of particle size variability were made due to skewed distribution. An alpha value of ≤ 0.05 was used to indicate statistically significant differences among the groups. All analyses were performed using a software program (SPSS™, Statistical Package for the Social Science, 11.5.1 Windows version, SPSS Inc. Chicago, Illinois).

3 Results

3.1 Reproducibility

The intra-examiner intraclass correlation coefficient (ICC) was 0.94 for particle size (in vitro study), 0.81 for tissue reaction (in vivo study) and 0.89 for cell counting.

3.2 Particle characterization

SEM analysis: biomaterials showed irregular particles with different surface characteristics. Group 1 (PerioGlas™) showed irregular particles, with some sharp-edged and others rounded. Particle surface was rough, suggesting the use of acid etching or crystallization, showing small round particles (0.5–1 μm) (Fig. 1a). Group 2 (Biogran™) had irregular and sharp granules with roughness suggesting use of acid etching or crystallization (Fig. 1b). Group 3 (BGU)

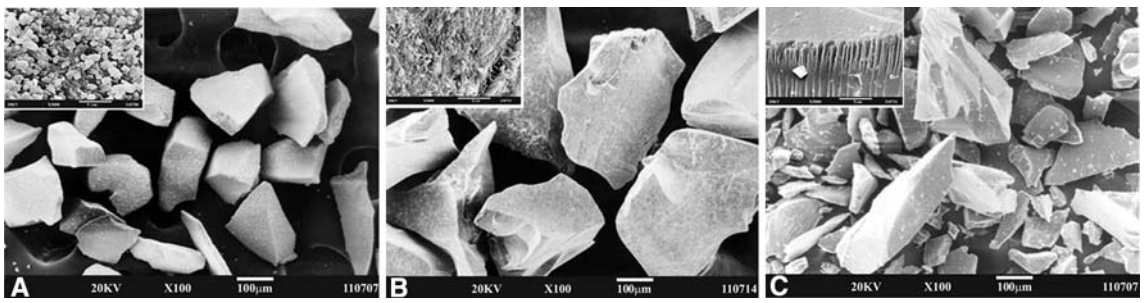

Fig. 1 SEM photomicrographs showing bioactive glasses granules shape and surface. (**a**) G1 (PerioGlas™) irregular and varied size particle (bar = 100 μm). (**b**) G2 (Biogran™) and (**c**) G3 (BGU) also showing irregular and varied size particle (bar = 100 μm). In detail it is possible to observe the roughness of the surface granules (bar = 5 μm)

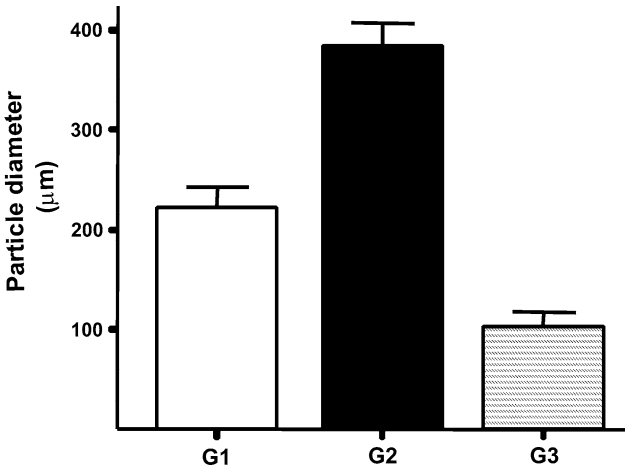

Fig. 2 Mean (standard deviation) particles diameter (μm) before implantation, G1 (PerioGlas™), G2 (Biogran™) and G3 (BGU)—statistically significant difference ($P < 0.0001$, ANOVA with Tukey post hoc test)

exhibited irregular sharp-edged particles with different sizes, showing a microrough and smoother surface (no chemical treatment) than the other groups (Fig. 1c). A statistically significant difference was observed among the groups for particle size (G1 = 222.0 ± 20.7 μm, G2 = 385.1 ± 21.9 μm and G3 = 102.9 ± 15.4 μm), $P < 0.0001$-ANOVA with Tukey post hoc test (Fig. 2 and Table 1).

Energy-dispersive X-ray (EDX), X-ray fluorescence (XRF) spectrometry, X-ray diffraction (XRD): EDX analysis showed calcium, oxygen, sodium, phosphorus and silicon in all groups. The major peaks of silicon were observed in the G1 and G2 (Fig. 3). XRF revealed silica oxide (SiO_2), sodium oxide (Na_2O), calcium oxide (CaO) and phosphorus oxide (P_2O_5). XRD spectrum indicated non crystalline phase for all the bioactive glasses tested (Fig. 4).

3.3 Biocompatibility analysis

All rats were healthy and did not present signs of edema or suppuration throughout the postoperative period.

7 days. All biomaterials showed erosion of the sharp edges of the resorbable glass granules. A mild inflammatory reaction consisting of polymorphonuclear and mononuclear inflammatory cells was observed around the particles in all groups. The connective tissue exhibited fibroblasts and fibrocytes with vascular proliferation. Control group (sham) had similar results to the experimental groups.

15 days. The connective tissue had similar characteristics with fibroblasts (Fs) and some fibrocytes. It was

Table 1 Descriptive statistics of particles' diameter (μm) of bioactive glasses samples in granular form determined by scanning electron microscope (MEV)

Biomaterials	Mean	SD	Percentiles					Min	Max
			10	25	50	75	90		
PerioGlas™	222.00	113.34	93.30	174.68	205.08	243.19	322.87	63.30	618.90
Biogran™	385.08	119.79	204.50	317.87	390.20	468.97	549.80	79.27	589.16
BGU	102.87	84.13	31.00	65.13	82.20	98.00	271.10	21.30	381.20

SD, standard deviation

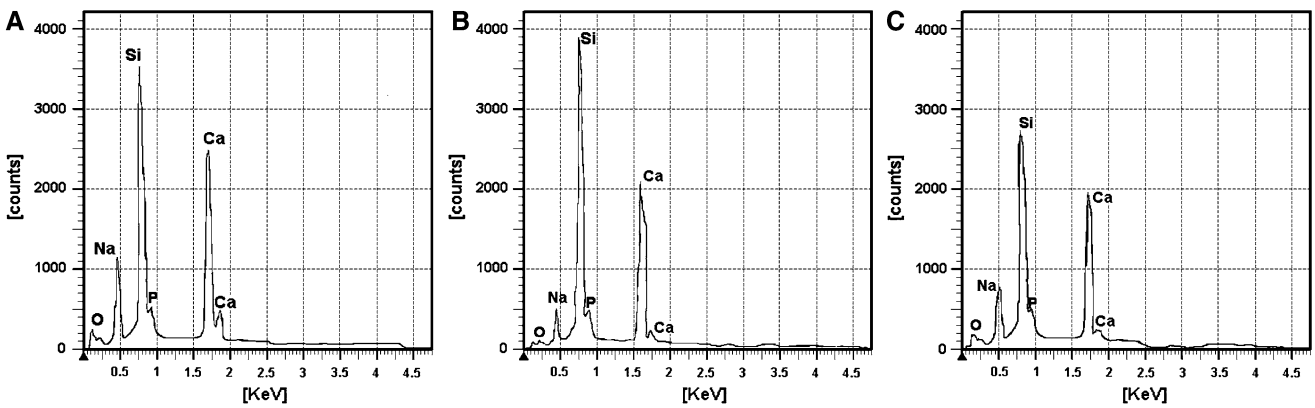

Fig. 3 EDX spectrum of materials granules in (**a**) G1 (PerioGlas™), (**b**) G2 (Biogran™) and 3C- G3 (BGU), demonstrating the presence of O (Oxygen), Na (Sodium), P (Phosphorus), Ca (Calcium) and Si (Silicon)

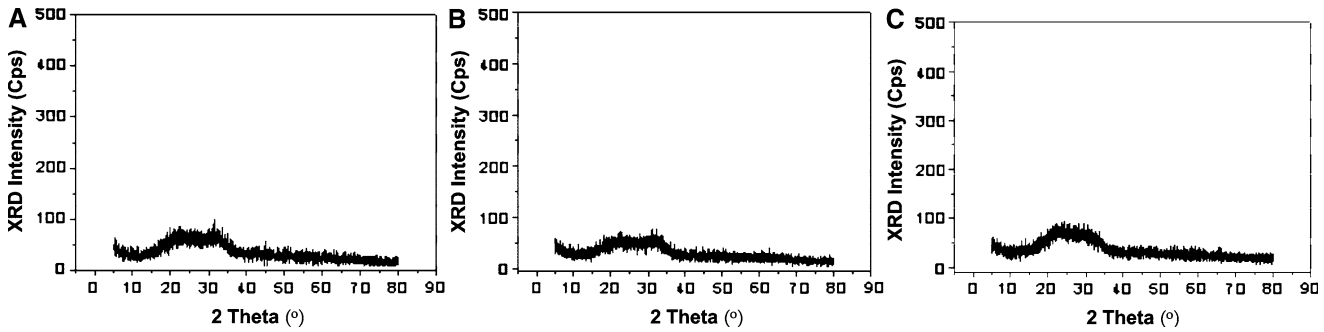

Fig. 4 XRD spectrum patterns in (**a**) G1 (PerioGlas™), (**b**) G2 (Biogran™) and (**c**) (BGU), none of the biomaterials were considered crystalline, similar patterns were found

observed edema and vascular proliferation, polymorphonuclears leukocyte (PMNs) and larger amount of mononuclears (MNs). The particles were surrounded by fibrous connective tissue, which consisted of densely packed collagen fibers with many inflammatory cells. The core of the particles started to disintegrate and fissures appeared (Fig. 5a). In the Control group (sham) few inflammatory cells were noted and the tissue showed a normal aspect (Fig. 5b).

21 days. In all groups the particles showed many fissures. The core of the granules seemed to have disintegrated and be replaced by organic components. The smaller particles showed much more disintegration than the larger ones. The disintegration was associated with numerous phagocytic cells. Particles in some specimens appeared encapsulated by collagen fibers, with the presence of PMN and MN cells observed. The Control group exhibited normal connective tissue, with intact muscle fibers and absence of a tissue reaction (Fig. 5c).

45 days. In all groups we observed PMNs, MNs, Fs, fibrocytes and blood vessels. Several particles were disintegrating and consequently splitting up into smaller parts. In most of the remaining granules the fissures had completely penetrated into the core. Connective tissue consisting of densely packed collagen fibers and fibroblasts was present around the fissures. A wide variation in the particle sizes was observed. The Control group continued to exhibit normal connective tissue, with absence of a tissue reaction with intact muscle fibers (Fig. 5d).

60 days. A large number of particles exhibited many fissures, a central disintegration, and excavation connecting to the surrounding tissues. Several particles were still surrounded by fibrous tissue. In all groups (tests and control) the connective tissue exhibited few PMN and MN cells. The population of fibroblasts in the fibrous tissue decreased gradually and the population of fibrocytes gradually increased after implantation (Fig. 5e, f).

A higher degree of tissue reaction was seen in group 3 (BGU) than in all the other groups at 15 and 21 days (statistically significant difference, $P < 0.01$). Similar results were observed for all experimental groups at 45 and 60 days, statistically with significant different from the Control group (Sham), ($P < 0.01$, Fig. 6).

A statistically significant difference was observed for percentage of PMNs, MNs and Fs among the groups ($P < 0.05$, ANOVA test) (Fig. 7a–c).

All biomaterials tested exhibited a reduction in particle size due to resorption, with a statistically significant difference among groups ($P < 0.05$, ANOVA) (Fig. 8).

4 Discussion

These experiments were conducted to investigate the Physical–chemical characterization and biocompatibility evaluation of three bioactive glasses. SEM evaluation exhibited irregular and non-uniform particle size. The particle size range indicated by manufacturer of the PerioGlas™ varies from 90 to 710 μm, whereas the particle size specified for the Biogran™ is from 300 to 360 μm. Discrepancies in particle size measurements between PerioGlas™ and Biogran™ manufacturers could be the result of the technique used for analysis. However, the relative measurement made in the present study yielded a valid comparison among the three biomaterials, since the same preprocessing and image analysis system were used to quantify the particles size [10]. Cancian et al. [1], showed that differences in granule size do not affect new bone formation. According to Silva et al. [20], spherical particles (210–350 μm) with smooth or rough surface have a non-cytotoxic behavior. Wheeler et al. [10] stated that smaller particles provide a greater surface area of bioactive glass, providing more sites for osteoblast adhesion and osseous formation. PerioGlas™ and Biogran™ have more uniform and regular particles, compared to the BGU. Granule surface may influence the biological response, improving protein adsorption [6, 7, 12]. Kaufmann et al. [6] suggested that porosity and roughness can affect

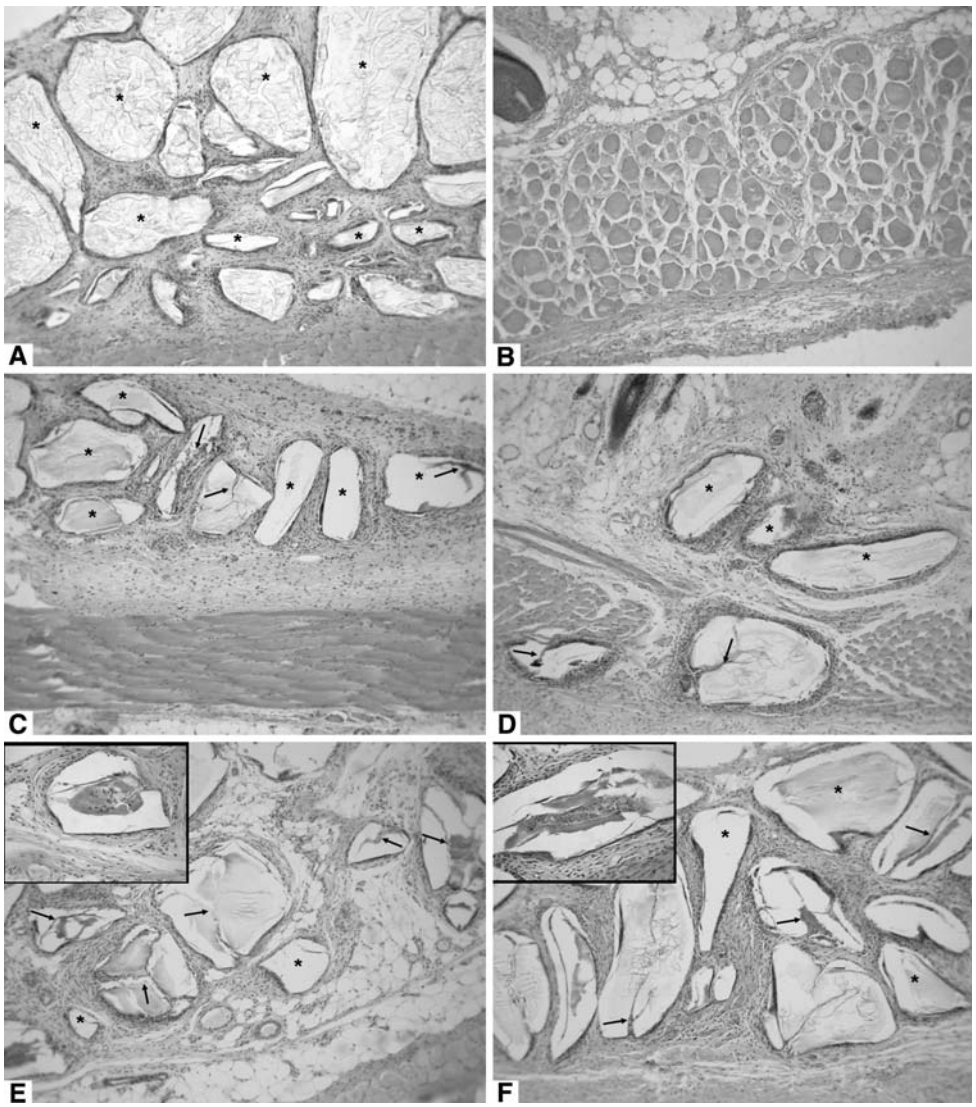

Fig. 5 Photomicrographs of materials implanted in rat tissue subcutaneous. (**a**) (15 days), Group 1 (PerioGlas^{TM}) particles (*) surrounded by fibrous tissue, the cores of the particles started to disintegrate and fissures appeared in some specimens. (b) (15 days), Group-4 (Control-Sham) exhibiting a normal connective tissue, absence of inflammatory response with intact muscle fibers. (**c**) (21 days), Group 2 (Biogran^{TM}) the core of the granules (arrows) appeared to have disintegrated and been replaced by organic components. Particles (*) encapsulated by collagen fibers with presence of PMNs and mononuclear cells. (**d**) (45 days), Group 2 (Biogran^{TM}) several particles (*) were disintegrating and consequently splitting up in smaller parts. In many of the remaining granules the fissures had completely penetrated to the core. Connective tissue was present among the fissures (arrows). (**e**) (60 days), Group 3-(BGU) and (**f**) Group 1 (PerioGlas^{TM}) particles (*) exhibited many fissures, a central disintegration (arrows). Original ×100 magnification. In detail it is possible to observe the central particle disintegration and excavation via a connection with the surrounding tissues (original ×400 magnification). Hematoxylin and eosin stain

cellular function. The particle surface was rough, suggesting the use of acid etching or crystallization in PerioGlas^{TM} and Biogran^{TM}. Superficial acid etching (hydrochloric acid) treatment of bioactive glass improves the biological properties. BGU exhibited microrough and smooth particles (no chemical treatment). Chemical acid etching selectively dissolved the apatite phase, which might also have formed a silica-gel layer by attacking the silicate phases and the residual glass. The increase in surface area caused by acid attack would render a more bioactive surface [11, 13].

Biomaterial resorption is directly related to the particle's size with the largest granules reabsorbed slower than the smaller ones. In guided bone regeneration procedures it is important that the biomaterial be reabsorbed simultaneously with osseous formation acting as a scaffold for osteogenesis [1–4, 10].

Chemical element composition and ratio can define the resorption grade (dissolution), crystallinity, osteoblast

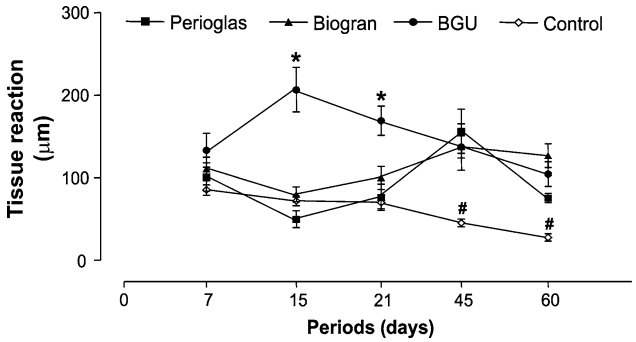

Fig. 6 Tissue reaction (μm) in the groups after experimental period (mean and standard error). 1. (*) statistically significant difference among BGU and the other groups after 15 and 21 days ($P < 0.01$). (#) statistically significant difference among control and all the other groups after 45 and 60 days ($P < 0.05$). ANOVA and Tukey post hoc test

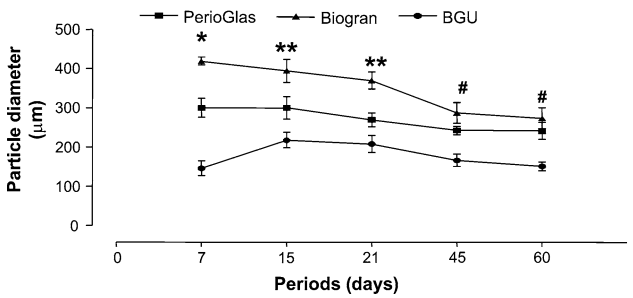

Fig. 8 Mean (Standard error) Particles diameter (μm) after subcutaneous. implantation. (*) statistically significant difference among the groups ($P < 0.01$). (**) Biogran™, statistically significant difference between BGU ($P < 0.01$). (**) Biogran™ statistically significant difference among the others groups ($P < 0.01$). (#) BGU, statistically significant difference among the others groups ($P < 0.05$). ANOVA with Tukey post hoc test

proliferation and many mechanical properties. Solid materials can be either crystalline or non crystalline (amorphous). Crystalline structures characterize the spatial form and atomic organization of the material. Highly crystalline biomaterials tend to be very insoluble, while poorly crystalline biomaterials have higher relative solubility. Crystalline biomaterials contribute little to the bone-like apatite formation in simulated body fluid [4, 8, 11, 12]. In the present study XRD showed an amorphous nature (non crystalline) for all the biomaterials. In accordance with the results of Roman et al. [13], the presence of crystalline phase can apparently be a hindrance to the bioactive behavior of glass-ceramics. Vitale-Baravone et al. [5] showed that the bioactive glass starts as an amorphous phase, but when in contact with physiological fluids, it undergoes ionic exchange, disappearing in the amorphous phase and appearing in the crystalline phase.

XRF and EDX revealed the presence of oxygen (O), sodium (Na), phosphorus (P), calcium (Ca) and silicon (Si) in all groups which formed silica oxide (SiO_2) sodium oxide (Na_2O), calcium oxide (CaO) and phosphorus oxide (P_2O_5). These results were similar to those of other studies [5, 8, 11, 20]. Chemical composition, dissolution process, crystallization degree, hydrophobicity, morphology and surface reactivity are factors that can influence the adsorption and protein expression of these biomateri+ als and consequently the biological properties [7, 21]. Bioactive glasses with similar formulations have been showing satisfactory results when used as bone substitutes [1–4, 9, 10, 17].

As for newly developed biomaterials, a biocompatibility screening must be performed as a preliminary step to determine the compatibility with biological systems. Synthetic grafts placed in the subcutaneous tissue of animals can be used to evaluate the in vivo compatibility of biomaterials in contact with connective tissues. The results of this method can be used as a preliminary source of information on the biocompatibility of different biomaterials [2, 3, 9, 16, 17].

Histologic results at 7 days showed resorbing glass granules and mild inflammatory reaction. At 15 days, the core of the particles had started to disintegrate and fissures

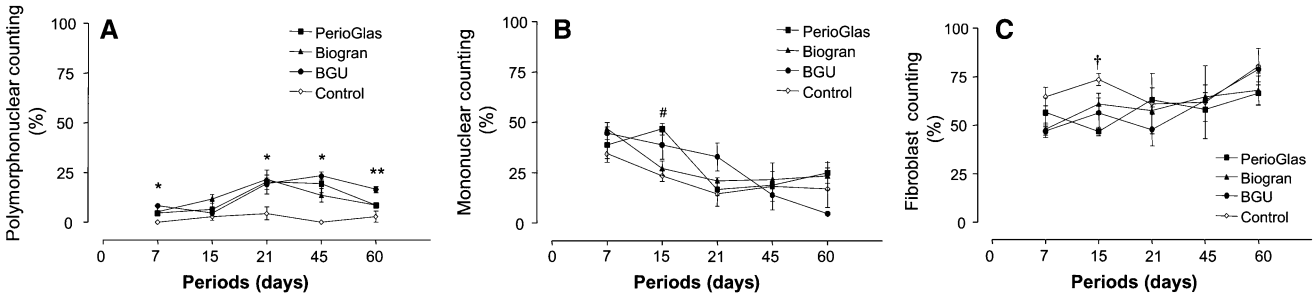

Fig. 7 Percentual cells counting in the groups after experimental period (mean and standard error). (**a**) Polymorphonuclear; (**b**) Mononuclerar and (**c**) Fibroblast. (*) statistically significant difference among control (Sham) and experimental groups ($P < 0.001$). (**) statistically significant difference beetwen BGU and PerioGlas™ ($P < 0.05$). (#) statistically significant difference among PerioGlas™, and Biogran™ and Control ($P < 0.05$). (†) statistically significant difference beetwen Control and PerioGlas™ ($P < 0.05$). ANOVA and Tukey post hoc test

appeared. In all groups the particles showed many fissures at 21 days. Several particles were disintegrating and consequently splitting up into smaller parts at 45 and 60 days and particle size varied greatly. Bioactive glasses in soft tissue were resorbed faster than in bone tissue, leading to dissolution of silicon into the local subcutaneous tissue [9, 16]. The silicon dissolved into the bloodstream, was filtered by the kidney, excreted in urine and removed from the body, thereby showing no accumulation in any major organs [16].

A number of particles were still surrounded by fibrous tissue. In all groups (test and control) the connective tissue exhibited few PMN and MN cells. Bosetti et al. [18] showed that PMN and MN cells respond to the biomaterial by increasing cytokine release and TNF-α expression. The cellular contact with biomaterials was sufficient to induce cell activation and release of cytokines. The population of fibroblasts in fibrous tissue decreased gradually and the population of fibrocytes increased gradually after implantation.

Measurement of tissue reaction was higher in the BGU than in other groups at 15 and 21 days. PerioGlas™ and Biogran™ had increased inflammatory reaction after 15 days; after this period, the initial resorption eliminated the effects of superficial treatment (acid etching- or hydrochloric acid), and then the tissue reaction was similar to the BGU. All biomaterials presented the same composition and concentration of chemical elements. Therefore, tissue reaction can be related to several factors such as: size, morphology, uniformity, and superficial characteristics [4, 6–8, 10, 12, 14, 15, 19, 20]. In addition, tissue reaction can be originated by direct contact with biomaterial, degradation of the small particles, and cellular contact with larger particles [9, 16, 18].

PerioGlas™ and Biogran™ have been used with success as bone substitutes in surgical procedures [2–4]. Cell counts (PMN, MN and F) were similar in all the experimental groups. These results are a favorable aspect of this new developed biomaterial (BGU).

In spite of the statistical significant difference among BGU and others groups at 15 and 21 days, the three biomaterials exhibited acceptable inflammatory response, being considered biocompatible and well tolerated by the tissues and inducing only a transitory inflammatory reaction, in accordance with other studies [1, 3, 4, 10, 17].

Biogran™ had larger particle size, followed by PerioGlas™ and BGU. PerioGlas™ and Biogran™ showed a reduction in particle size from 7 to 60 days. BGU had a particle size increase from 7 to 21 days, and a reduction from 21 to 60 days. These findings occur because small particles are resorbed faster than larger ones. Vogel et al. [17], implanted bioactive glass in a femoral site and found a reduction in the particle diameter. Bioactive glasses are partially resorbable when implanted in osseous and soft tissues [1–4, 9, 10, 17].

Bioactive glasses implanted in osseous and soft tissues exhibit fissures, cracks, and core dissolution within the particles. It is suggested that this phenomenon arises as follows: the interfacial ion exchange between the glass particles and the surrounding tissue fluids results in the formation of Si-rich gel which extends throughout the core of particle. This extensive gelation is possible given the particle size and the high fluid turnover due to the high vascularity of the tissue. At the same time, a CaP-rich layer is formed on the outer surface of the particle and covers the Si-rich gel. Phagocytic cells penetrate this Si-rich gel via small cracks in the Ca-P rich layer and start the resorption of the gel. Subsequent to the resorption, mesenchymal cells penetrate via the small ducts between the excavated center and the surrounding tissues [1, 9]. Bioactive glass dissolution causes intra- and extra-cellular alkalinization and raises [Ca^{2+}] which can stimulate osteoblast ATP production. These properties may produce an environment which stimulates bone growth [12, 15].

In this study, fissures and cracks in the particles were observed in all biomaterials at 15 days. Extensive particle degradation was observed at 45 and 60 days, with many fissures and cracks filled by connective tissue with the granule core showing signs of excavation. Vogel et al. [17], did not observe cracks in bioactive glass at 7 days (femoral sites), but at 28 days, clefts were found through the particles. Wheeler et al [10], found some cracked particles at 12 weeks (femoral sites), with pouches developed primarily in particles >300 μm in diameter, which were also seen in smaller particles. Infiltration cracks and internal pouches may hasten the resorption of the graft material, increasing the surface exposure area to the physiological environment.

In conclusion, the experimental bioactive glass analyzed showed physical and chemical characteristics similar to the commercially by available biomaterials, and was considered biocompatible, being partially reabsorbed in the subcutaneous tissue.

Acknowledgements This work was supported by Coordenação de Aperfeiçoamento de Pessoal de Nível Superior (CAPES), Brazil.

References

1. D.C. Cancian, E. Hochuli-Vieira, R.A. Marcantonio, I.R. Garcia Junior, Utilization of autogenous bone, bioactive glasses, and calcium phosphate cement in surgical mandibular bone defects in Cebus apella monkeys. Int. J. Oral Maxillofac. Implants **19**, 73 (2004)
2. A. El-Ghannam, H. Amin, T. Nasr, A. Shama, Enhancement of bone regeneration and graft material resorption using surface-

modified bioactive glass in cortical and human maxillary cystic bone defects. Int. J. Oral Maxillofac. Implants **19**, 184 (2004)
3. T. Turunen, J. Peltola, A. Yli-Urpo, R.P. Happonen, Bioactive glass granules as a bone adjunctive material in maxillary sinus floor augmentation. Clin. Oral Implants Res. **15**, 135 (2004)
4. K.A. Al Ruhaimi, Bone graft substitutes: a comparative qualitative histologic review of current osteoconductive grafting materials. Int. J. Oral Maxillofac. Implants **16**, 105 (2001)
5. C. Vitale-Brovarone, E. Verne, M. Bosetti, P. Appendino, M. Cannas, Microstructural and in vitro characterization of SiO2–Na2O–CaO–MgO glass-ceramic bioactive scaffolds for bone substitutes. J. Mater. Sci. Mater. Med. **16**, 909 (2005)
6. E.A. Kaufmann, P. Ducheyne, I.M. Shapiro, Effect of varying physical properties of porous, surface modified bioactive glass 45S5 on osteoblast proliferation and maturation. J. Biomed. Mater. Res. **52**, 783 (2000)
7. E.A. Kaufmann, P. Ducheyne, I.M. Shapiro, Effect of varying physical properties of porous, surface modified bioactive glass 45S5 on osteoblast proliferation and maturation. J. Biomed. Mater. Res. **52**, 783 (2000)
8. S.B. Cho, F. Miyaji, T. Kokubo, T. Nakamura, Induction of bioactivity of a non-bioactive glass-ceramic by a chemical treatment. Biomaterials **18**, 1479 (1997)
9. E. Schepers, L. Barbier, P. Ducheyne, Implant placement enhanced by bioactive glass particles of narrow size range. Int. J. Oral Maxillofac. Implants **13**, 655 (1998)
10. D.L. Wheeler, K.E. Stokes Ke, R.G. Hoellrich, D.L. Chamberland, S.W. Mcloughlin, Effect of bioactive glass particle size on osseous regeneration of cancellous defects. J. Biomed. Mater. Res. **41**, 527 (1998)
11. A.J. Salinas, J. Roman, M. Vallet-Regi, J.M. Oliveira, R.N. Correia, M.H. Fernandes, In vitro bioactivity of glass and glass-ceramics of the 3CaO × P2O5–CaO × SiO2–CaO × MgO × 2SiO2 system. Biomaterials **21**, 251 (2000)
12. I.A. Silver, J. Deas, M.M. Erecinska, Interactions of bioactive glasses with osteoblasts in vitro: effects of 45S5 Bioglass, and 58S and 77S bioactive glasses on metabolism, intracellular ion concentrations and cell viability. Biomaterials **22**, 175 (2001)
13. J. Roman, A. J. Salinas, M. Vallet-Regi, J.M. Oliveira, R.N. Correia, M.H. Fernandes, Role of acid attack in the in vitro bioactivity of a glass-ceramic of the 3CaO.P2O5–CaO.SiO2–CaO.MgO.2SiO2 system. Biomaterials **22**, 2013 (2001)
14. A. Itälä, V.V. Välimäki, R. Kiviranta, H.O. Ylanen, M. Hupa, E. Vuorio, H.T. Aro, Molecular biologic comparison of new bone formation and resorption on microrough and smooth bioactive glass microspheres. J. Biomed. Mater. Res. B Appl. Biomater. **65**, 170 (2003)
15. M. Cerruti, D. Greenspan, K. Powers, Effect of pH and ionic strength on the reactivity of Bioglass 45S5. Biomaterials **26**, 1665 (2005)
16. W. Lai, J. Garino, C. Flaitz, P. Ducheyne, Excretion of resorption products from bioactive glass implanted in rabbit muscle. J. Biomed. Mater. Res. A **75**, 398 (2005)
17. M. Vogel, C. Voigt, U.M. Gross, C.M. Muller-Mai, In vivo comparison of bioactive glass particles in rabbits. Biomaterials **22**, 357 (2001)
18. M. Bosetti, L. Hench, M. Cannas, Interaction of bioactive glasses with peritoneal macrophages and monocytes in vitro. J. Biomed. Mater. Res. **60**, 79 (2002)
19. T. Wilson, V. Parikka, J. Holmbom, H. Ylanen, R. Penttinen, Intact surface of bioactive glass S53P4 is resistant to osteoclastic activity. J. Biomed. Mater. Res. A **77**, 67 (2006)
20. G.A. Silva, F.J. Costa, O.P. Coutinho, S. Radin, P. Ducheyne, R.L. Reis, Synthesis and evaluation of novel bioactive composite starch/bioactive glass microparticles. J. Biomed. Mater. Res. A **70**, 442 (2004)
21. C. Knabe, M. Stiller, G.F. Berger, D. Reif, R. Gildenhaar, C.R. Howlett, H. Zreiqat, The effect of bioactive glass ceramics on the expression of bone-related genes and proteins in vitro. Clin. Oral Implants Res. **16**, 119 (2005)